CONF-8910225--3

ICRF FARADAY SHIELD PLASMA SHEATH MODELS: LOW AND HIGH CONDUCTIVITY LIMITS

J. H. Whealton, P. M. Ryan, and R. J. Raridon,
Oak Ridge National Laboratory, Oak Ridge, TN 37831

CONF-8910225--3

DE90 001757

ABSTRACT

Using a 2-D nonlinear formulation which explicitly considers the plasma edge near a Faraday shield in a self consistent manner, progress is indicated in the modeling of the ion motion for a Faraday shield concept and model suggested by Perkins. Several models are considered which may provide significant insight into the impurities generation for ICRH antennas.

INTRODUCTION

Ion Cyclotron Heating (ICH) at high power densities (5-10 kW/cm^2) offers several challenges–one of which is the anticipated high rates of heavy metal impurity generation and outflux. An understanding of the plasma edge near such antennas is an important part of eliminating or mitigating this problem. The present work reports progress toward this understanding.

The plasma edge problem presents formidable difficulties of treatment, particularly near the ICH antenna. One difficulty is the extreme nonlinearity of the equations describing the plasma sheath for an edge plasma on the order of 10^{11}/cm^3. A second is the dimensionality involved; the complex geometry near an ICH antenna, with a Faraday shield and local limiters, demands the imposition of 3D boundary conditions. A third is the time scales involved; an accurate model may need to account for electron motion in the magnetized plasma over short electron time scales, ion motion over many rf/ion cyclotron periods, and impurity distribution evolution over long, quasi-steady state periods. The model also needs to connect with the properties of the bulk plasma, preferably in an iterative, self-consistent manner.

MATHEMATICAL FORMULATION

From the Fokker-Planck-Maxwell equations (in Lorentz gauge):

$$\left[\frac{\partial}{\partial t} + \mathbf{v}\cdot\nabla_r + \frac{q_i}{m_i}\mathbf{a}_i\cdot\nabla_v\right] f_i\,(\mathbf{r},\mathbf{v},t) = \beta\, g\,(\mathbf{r},\mathbf{v},t) \qquad (1)$$

MASTER

*Research sponsored by the Office of Fusion Energy, U.S. Department of Energy, under contract DE-AC05-84OR21400 with Martin Marietta Energy Systems, Inc.

$$\nabla^2\phi - \frac{1}{c^2}\frac{\partial^2\phi}{\partial t^2} = -\sum_i f_i\,(v)\,dv \tag{2}$$

$$\nabla^2\mathbf{A} - \frac{1}{c^2}\frac{\partial^2 A}{\partial t^2} = -\sum_i \mathbf{v}\,f_i\,(v)\,dv \tag{3}$$

where

$$\mathbf{E} = -\nabla\phi - \frac{1}{c}\frac{\partial\mathbf{A}}{\partial t}, \quad \mathbf{B} = \nabla \times \mathbf{A}. \tag{4}$$

We will concentrate on the equation for the scalar potential, ϕ, Eq. (2). If one considers distances on the order of a Debye length, then the time derivative term is approximately six orders of magnitude smaller than the other terms at ion cyclotron frequencies (Debye length much smaller than free space wavelength).

Equation (3) will be considered separately from this analysis for example, from a solution of the homogeneous Helmholtz equation in 3-D [Ref. 1] or in at least 2-D [Ref. 2] or the 3-D scalar magnetostatic models, $\nabla^2\Psi = 0$ [Ref. 3], where Ψ is the magnetostatic potential.

The dynamical equation, Eq. (1), (Fokker-Planck) for a single species ion distribution function $f_i(v,r,t)$ is considered with the remnants of Eq. (2), and the acceleration, $\mathbf{a}$ (r,v,t), contributions appropriate to the region near a Faraday shield.

$$\left\{\frac{\partial}{\partial t} + \mathbf{v}\bullet\nabla_r + \frac{q}{m}\left[\mathrm{v}\times(\mathbf{B}_0 + \nabla\times\mathbf{A}) - \nabla\phi - \frac{1}{c}\frac{\partial\mathbf{A}}{\partial t}\right]\bullet\nabla_v\right\} f(\mathbf{r},\mathbf{v},t) = \beta g(\mathbf{r},\mathbf{v}) \tag{5}$$

$$\nabla^2\phi(\mathbf{r},t) = -4\pi\left\{N_{eo}\exp\left[e\big(\phi(\mathbf{r},t) - \phi_p(\mathbf{r},t)\big)/kT\right] - \int dv\, f(\mathbf{r},\mathbf{v},t)\right\}, \tag{6}$$

where $\mathbf{B}_0$ is a constant applied toroidal magnetic field, $\mathbf{A}$ is the sinusoidally varying solution to (3), and a Boltzmann distribution is assumed for the electrons.

The nonlinear formulation of Eqs. (5)-(6) constitutes a self-consistent description of: the sheath potentials, the onset of charge separation in the plasma, ponderomotive forces, ion Bernstein wave launching and damping, ion acoustic waves, edge plasma ion turbulence, sheath rectification, charged impurity ejection, and a whole host of near field phenomena, many of which are probably undiscovered at this point, but may be important. This formulation has been used routinely for long time scale sheath problems in the past [Ref. 4-5].

HIGH PLASMA CONDUCTIVITY (CONDUCTIVE) MODEL

An example and model that will be considered is that of Perkins [Ref. 6]. By use of Faraday's law one considers a time dependent boundary value problem on the scalar potential such as shown in Fig. 1. In the metallic elements **E** is assumed zero and thus (in Lorentz gauge) $\nabla\phi = -(1/c)\,\partial A/\partial t$. It turns out that the $(1/c)\,\partial A/\partial t$ forces are negligable on the scale of Bo at least over 10 rf cycles but we include it anyway. We will extend Perkins' analysis to two dimensions.

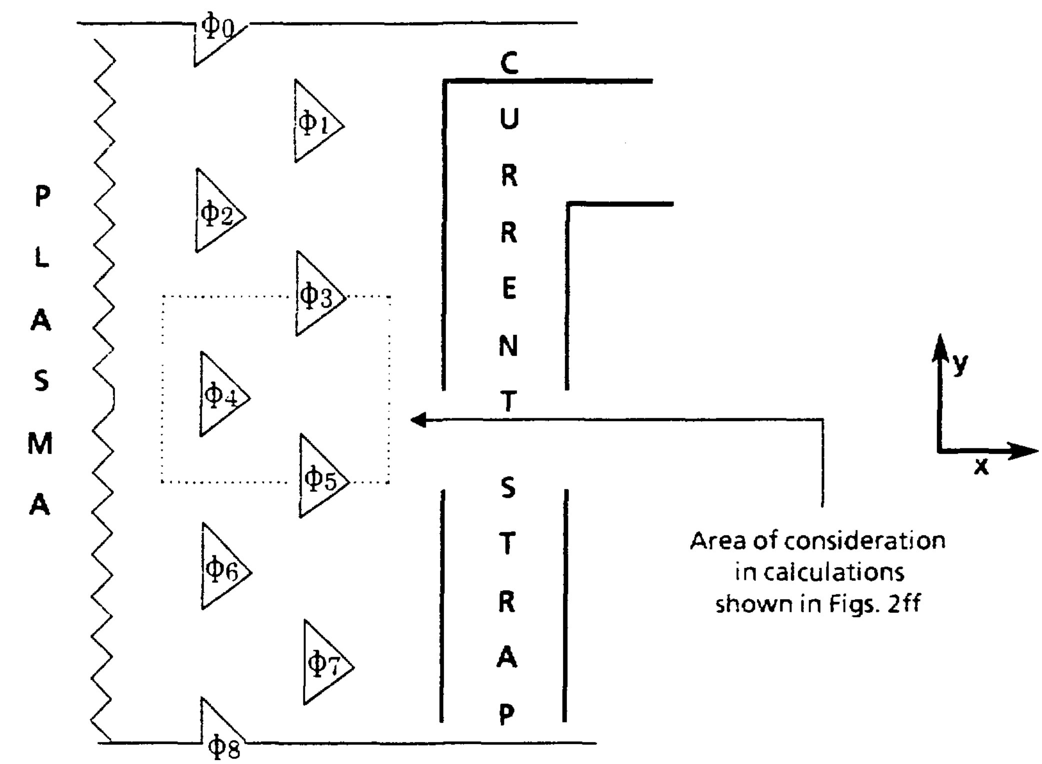

FIG. 1

As an illustrative calculation, we assume an immobile ion density in steady state for a case where the plasma potential, ϕ_p (**r**, t), is spatially uniform and is equal to ϕ_5, the maximum potential considered as shown in Fig. 2.

Figure 2 shows electrostatic equipotential contours which are the solution of

$$\nabla^2\phi(r) = -4\pi N_{eo}\left\{exp\left[e(\phi(r) - \phi_p)/kT\right] - 1\right\} . \tag{7}$$

these equipotentials are denoted by dashed lines. The contours are placed at equal intervals except for the last six controus which are exponentially placed. These stretch out into the presheath region. The transition is indicated by the heavy dashed line. The blank places in the middle are the quiescent plasma at a plasma potential of ϕ_5. Note that $|\phi_5 - \phi_4| >> kT_e/e$.

This is a subgroup of the class of zero resistivity problems where the time dependent plasma potential $\phi_p(r,t)$ is locked to an adjacent boundary along a magnetic field. The potential ϕ_4 is halfway between ϕ_3 and ϕ_5. It is the intention of this configuration that there would be sheath fields only on the right-hand side of the ϕ_4 electrode, so that sputtered material would go into the antenna or Faraday shield region as opposed to entering the confinement plasma. The presence of sheath fields on the left-hand side of the electrode is due to the imposition of the plasma potential $\phi_p(t)$, with respect to that electrode potential. Therefore, we can see that the model and the results are very much dependent upon the local plasma potential.

Ion trajectories and equipotentials from the solution to the time-dependent Eqs. (5)-(6) during a small interval are shown in Fig. 3. A uniform ion generation rate has been assumed. The phase of the RF cycle is the same as the steady state case considered in Fig. 2. The ions are uniformally generated. Lines attached to the (square) ion locations indicate the velocity of ions. As can be seen, the ions near the surfaces move with relatively high speed compared with those in the (largely shielded) plasma. The evolution of about 30,000 trajectories is shown in Fig. 4 over 10 rf cycles. Again, most of the action is near the Faraday shield elements. An energy distribution function of ions intercepting the ϕ_4 electrode is shown in Fig. 5 by the square symbol. A peak occurs at several times kT_e/e. Also shown is the energy distribution of the ions which remain in the region. Virtually all (99%) of these ions ha e energies less than kT_e/e.

LOW PLASMA CONDUCTIVITY (RESISTIVE) MODEL

In this case the plasma is considered to be perfectly neutral corresponding to the electrons inability to conduct along magnetic field lines on the time-space scales involved.. The ion trajectories are shown in Figure 6-7 in analogue with the conductiove model case of Fig. 3-4. The absence of a plasma makes for a lower mean energy for incident ions as can be seen by comparing Fig. 4 with Fig. 7. This is because the peak fields are generally lower in this limit as compared to the conductiove limit. The strong sheath fields, shown in Figs. 2 or 3, are not present in this limit: Fig. 6. The ion trajectories integrated over 10 full rf cycles are shown in Fig. 7. As can be seen the ion energies are less than that of the corresponding limit, Fig. 4, where through conduction, a plasma potential is maintained.

In fact, less than 1% of the ions reach an energy of kTe/e during their jitter-even those that hit the ϕ_4 Faraday shield.

Just to show how important the plasma space charge imbalance is, a completely non-neutral plasma (no electrons but the same 3 x $10^{10}/cm^2$ ion density) is considered. As can be seen in Fig. 8, the space charge fields completely dominate the induction fields and the ions all rocket to the Faraday shield at very high energy (Fig. 9).

CONCLUSIONS

The models here suggest that the conductive model predicts high ion impact energy on the Faraday shield elements (on the order of the induced potentials) the resistive model on the other hand produces much lower impact energies. The model of even this weak plasma (3 x 10^{10}/cc) is very important..

The results herein are to be considered as preliminary in several respects: (1) There are ambiguities in the plasma potential which are an important feature of the conductive model. This can be partially resolved by a full 3-D treatment of the boundary conditions; alternatively, plasma potentials may be imposed by geometrical consideration along a magnetic field line in conjunction with Faraday's law. (2) Numerical stability and variation of parameters' consistency have not yet been fully established. The status of ion acoustic-like waves routinely found in the solutions are not yet validated.

ACKNOWLEDGEMENTS

We wish to thank P. S. Meszaros, K. E. Rothe, W. R. Becraft, J. F. Cox, E. G. Elliott, and H. H. Haselton for their help and assistance. We wish to also thank F. W. Perkins (at PPPL) for his suggestions and M. Carter for suggesting that low and intermediate conducting cases may be important.

REFERENCES

1. J. H. Whealton, G. L. Chen, R. J. Raridon, R. W. McGaffey, E. F. Jaeger, M. A. Bell, D. J. Hoffman, *J. Comput. Phys.*, **75**, 168-189 (1987).
2. E.F. Jaeger, D. B. Batchelor, H. Weitzner, J. H. Whealton, *Computer Physics Communications* **40**, 33 (1986).
3. P. M. Ryan, K. E. Rothe, J. H. Whealton, D. W. Swain. 8th Topical Conference on Radio Frequency Power in Plasmas, Irvine, California, May 1-3, 1989, also see preceeding paper.
4. J. H. Whealton, R. W. McGaffey, P. S. Meszaros. *J. Comput. Phys.* **63**, 20 (1986); "Ion Optics Arithmetric," J. H. Whealton, Nucl. Instrum. Meth. 189, 55 (1981); "Space Charge Ion Optics Including Extraction from a Plasma," J. H. Whealton and J.C. Whitson; Particle Accelerator, 10, 235 (1980)
5. J. H. Whealton, R. J. Raridon, M. A. Bell. NATO/ASI on High Brightness Accelerators, Pitlochry, Scotland, 1986; "Computer Modeling of Negative Ion Beam Formation," J. H. Whealton, M. A. Bell, R. J. Raridon, K. E. Rothe, and P. M. Ryan, J. Appl. Phys. 64, 6210 (1988).
6. F. W. Perkins, PPPL Report #2571 (1988).

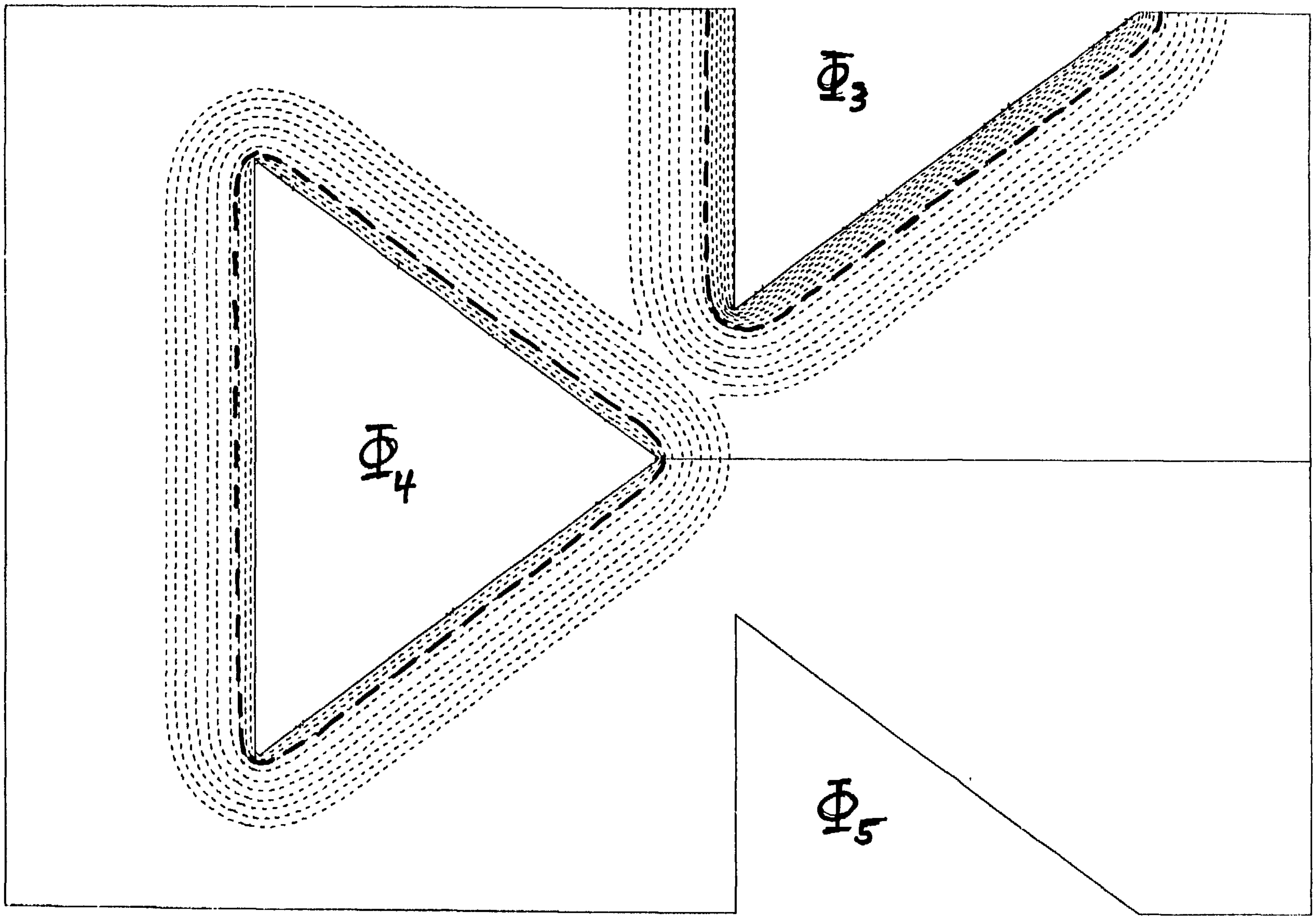

FIG 2

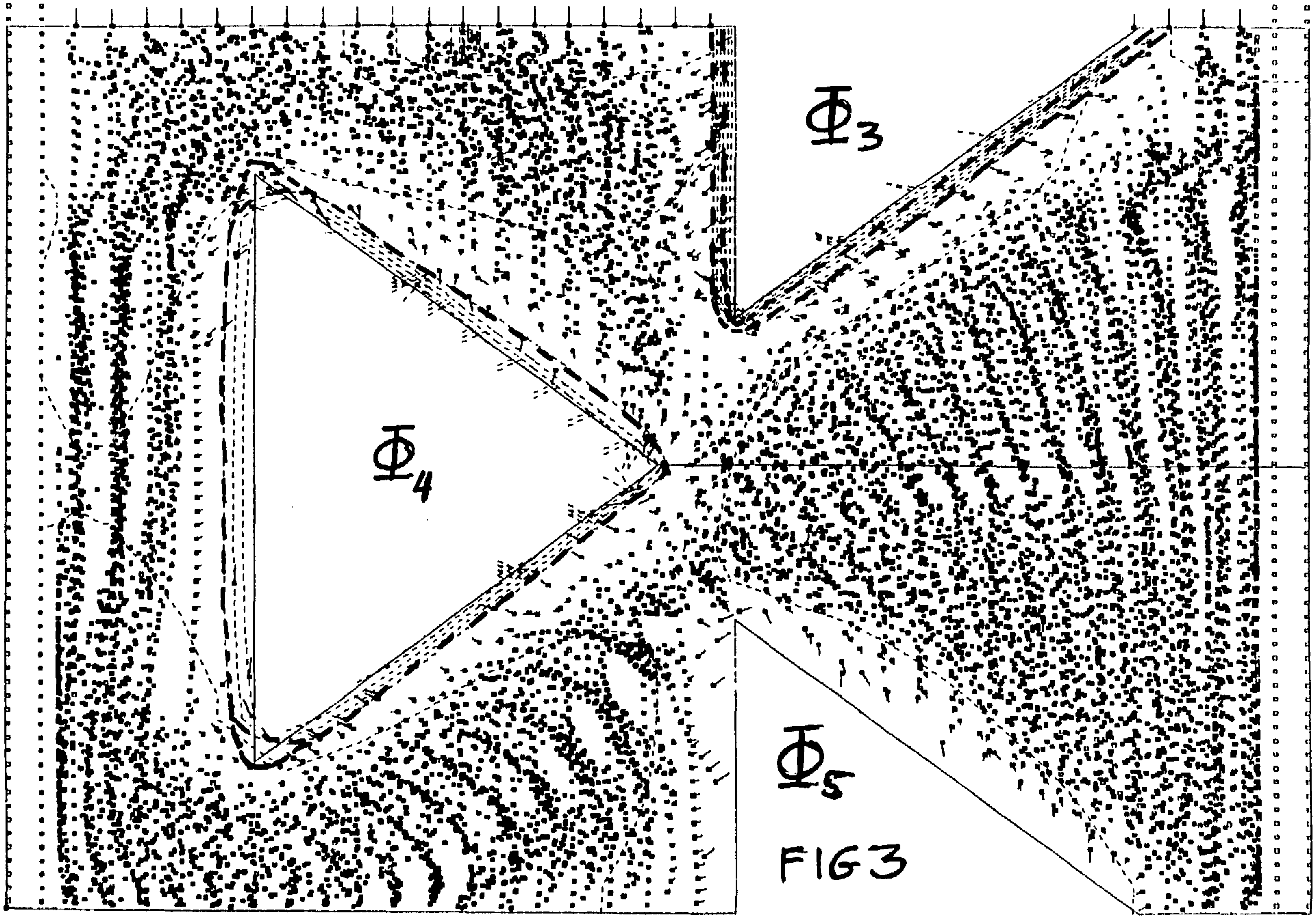

FIG3

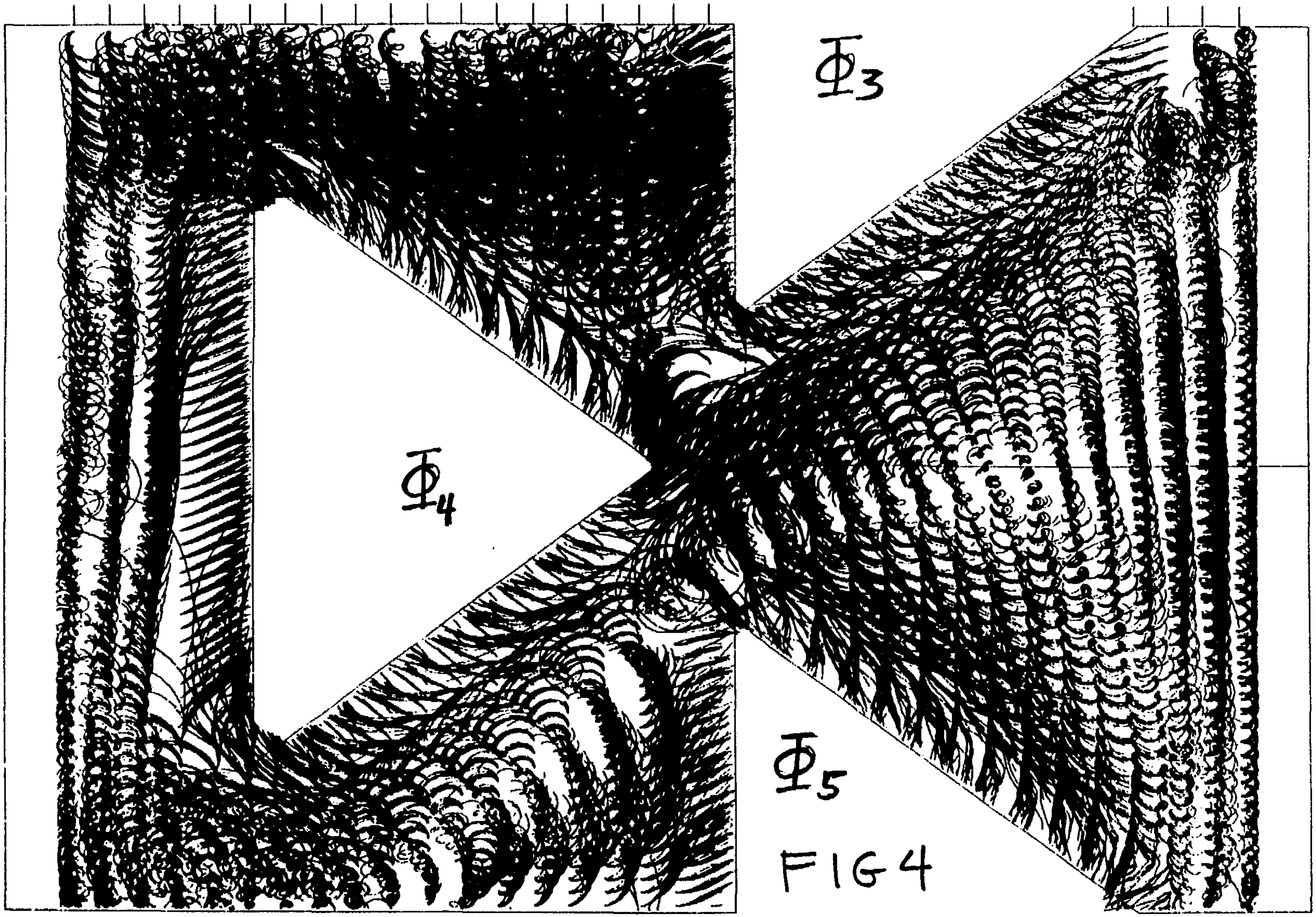

FIG 4

PLOT 1 11.07.25

PLOT.SAV18

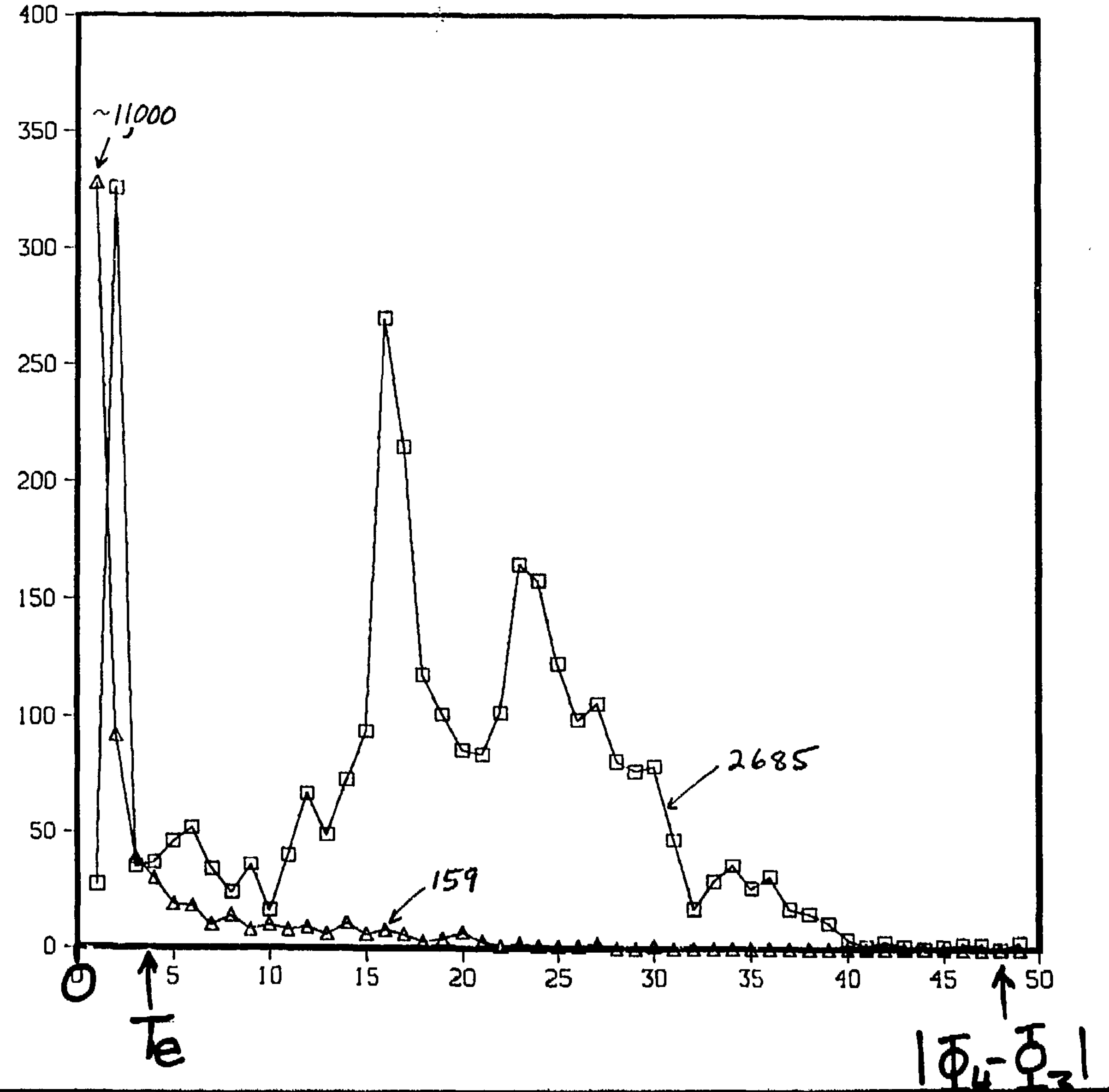

FIG5

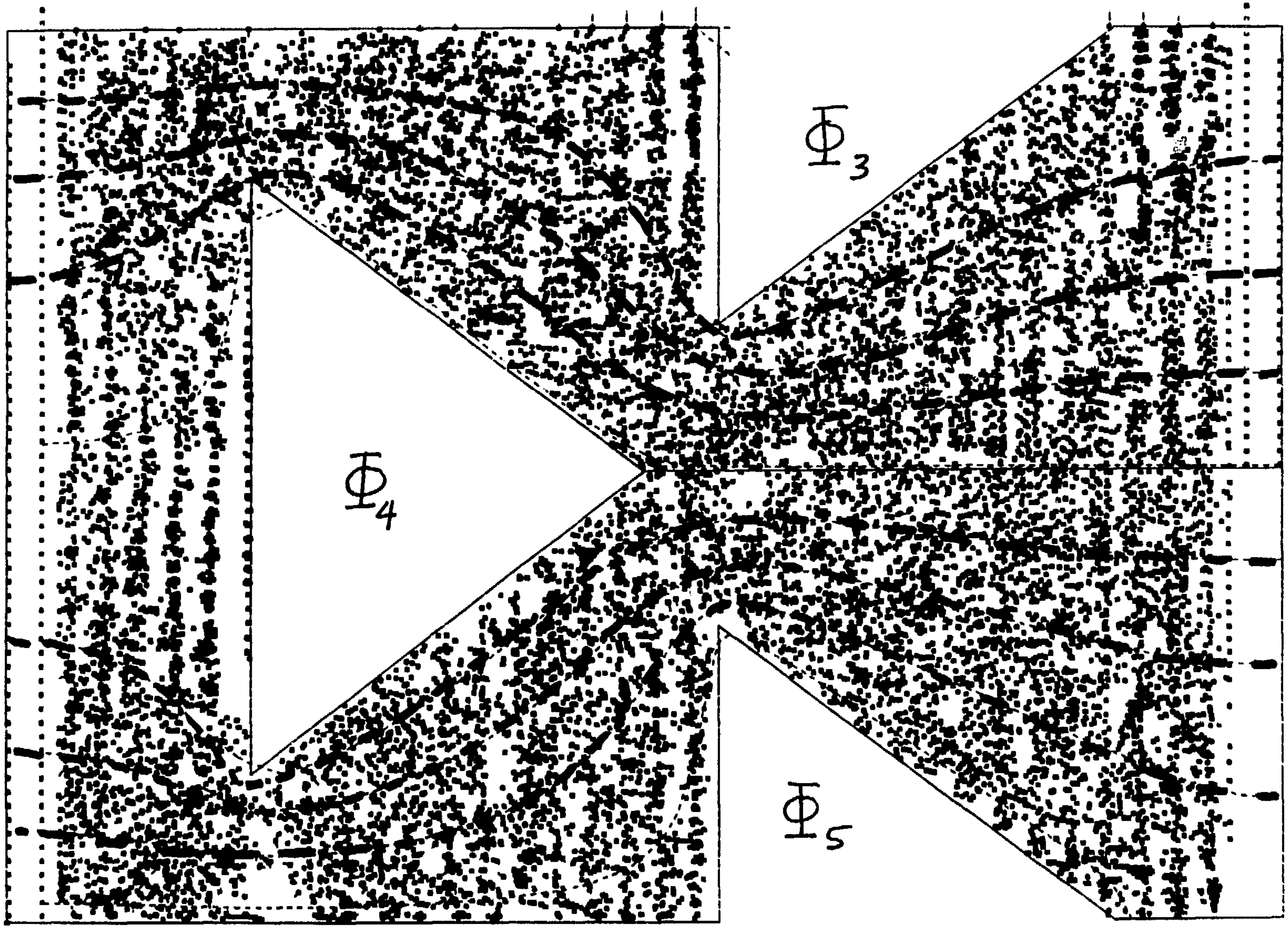

PLOT 80 03:36:14

GL86

PLOT 80 05.19.54

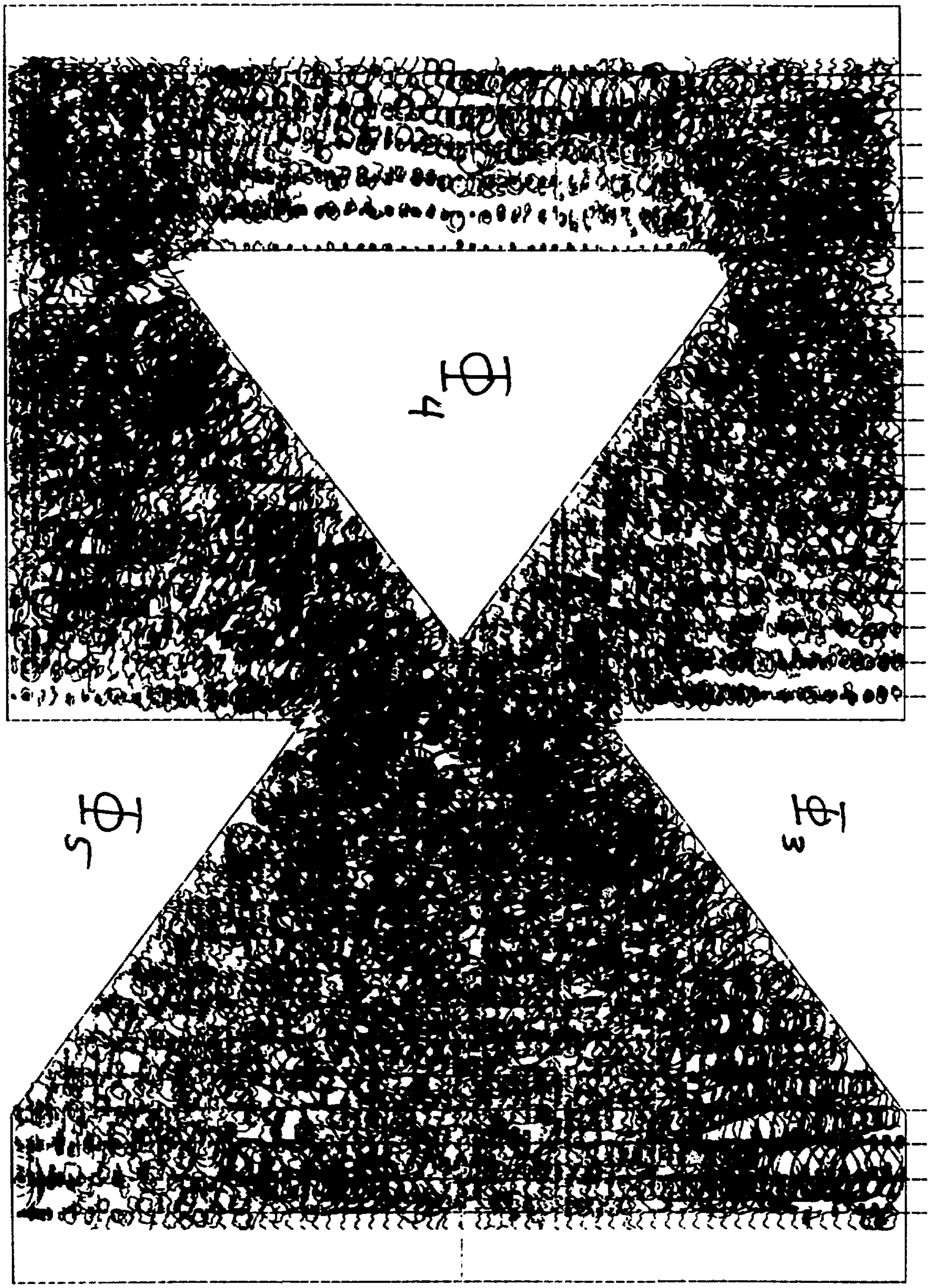

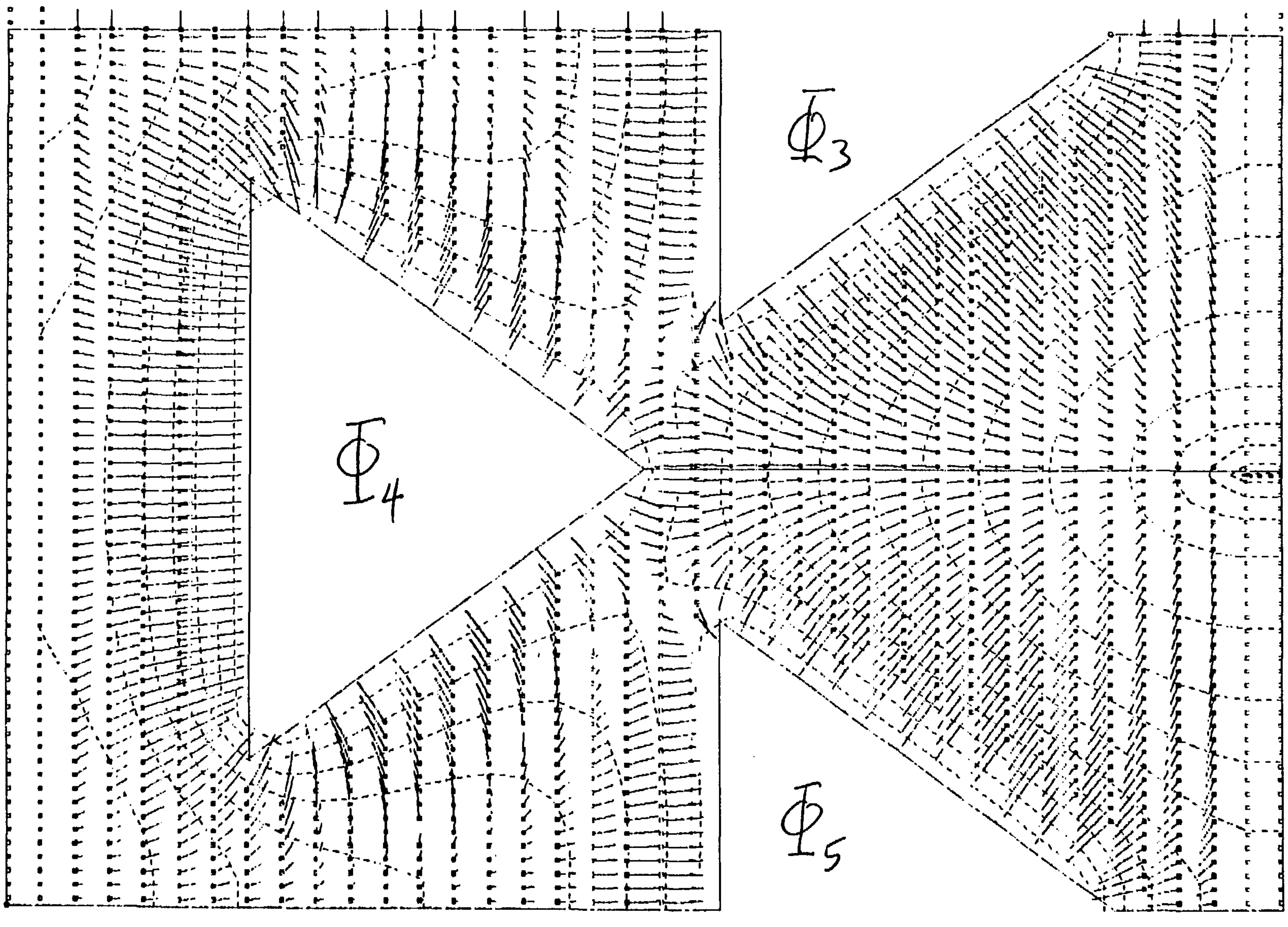

FIG 8

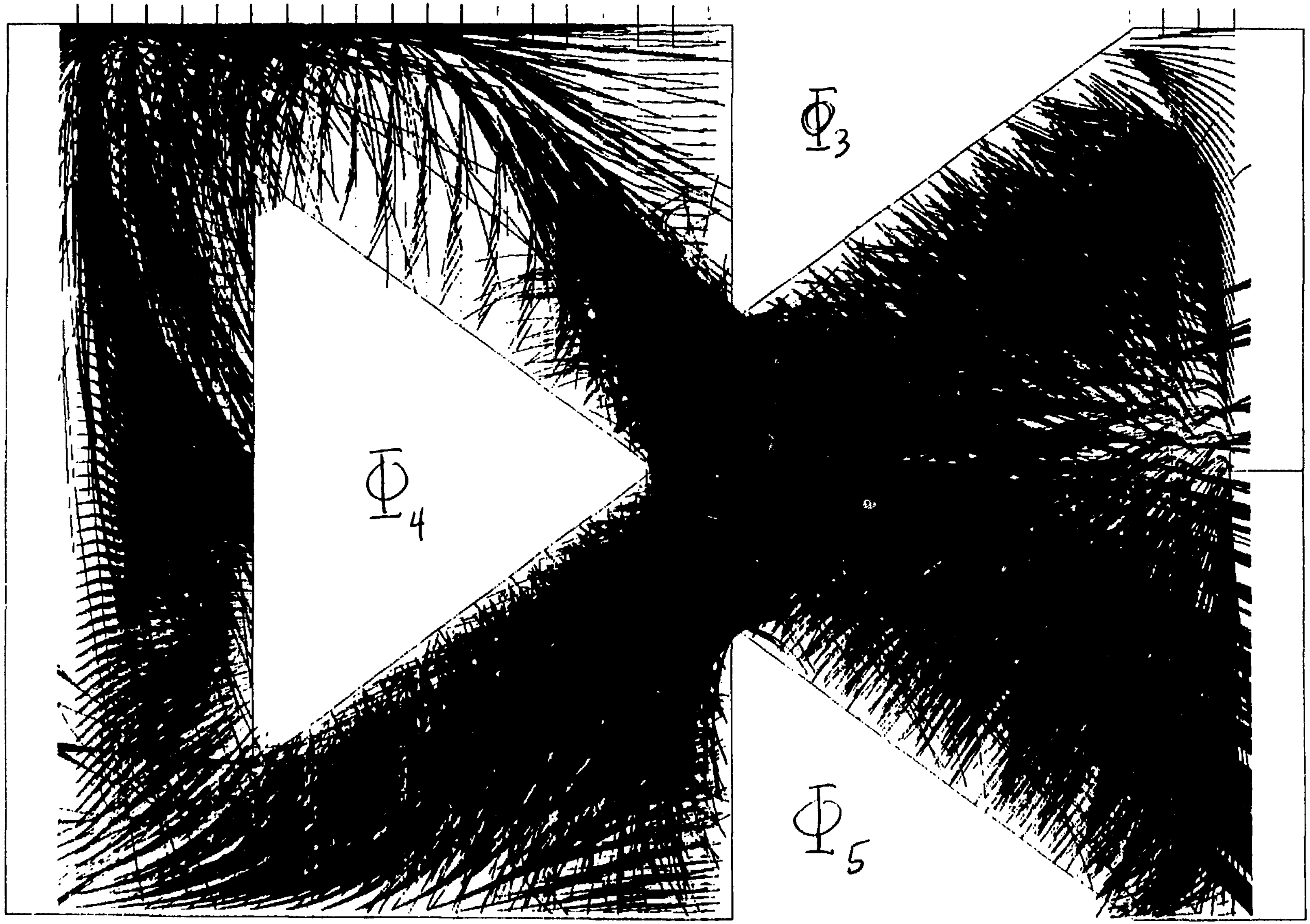

FIG. 9